Acta Universitatis Carolinae. Mathematica et Physica

B. Smola

Precipitation and hardening mechanisms in the AISI 321 steel

Acta Universitatis Carolinae. Mathematica et Physica, Vol. 31 (1990), No. 1, 27--46

Persistent URL: http://dml.cz/dmlcz/142613

Precipitation and Hardening Mechanisms in the AISI 321 Steel

B. SMOLA

Praha*)

Received 10 May 1989

Precipitation in austenitic Ti stabilized stainless steel AISI 321 has been studied by means of transmission electron microscopy and electron diffraction of thin foils. Structure, arrangement shape, size and density of precipitates was determined in dependence on thermal and mechanical treatment of polycrystalline steel specimens. The contributions of single hardening processes to the strength σ are evaluated from experimental results using theoretical models for hardening processes involved. Comparing with experimentally determined proof stress $\sigma_{0.2}$ at 350 °C the combination of single contributions is tested.

Byl studován průběh precipitace v austenitické chromniklové oceli stabilizované titanem AISI 321 (ČSN 17247). Pomocí transmisní elektronové mikroskopie a difrakce elektronů na tenkých foliích byly určeny uspořádání, tvar, velikost a hustota vyprecipitovaných fází a jejich struktura v závislosti na tepelném a mechanickém zpracování polykrystalických vzorků oceli. Na základě teoretických modelů různých zpevňovacích mechanismů jsou z naměřených hodnot vypočteny velikosti příspěvků k celkové pevnosti σ a srovnáním s experimentálně stanovenou smluvní mezí kluzu $\sigma_{0.2}$ při teplotě 350 °C testován způsob kombinace těchto jednotlivých příspěvků.

Исследовалось выделение дисперсных фаз в хромоникелевой нержавеющей аустенитической стали типа AISI 321 (ГОСТ ОХ18Н10Т) стабилизированной титаном. При помощи трансмиссионной электронной микроскопии и дифракции электронов в тонких фольгах была установлена зависимость структуры, распределения, вида, величины и плотности частиц фаз выделения от условий термической и механической обработок поликристаллических образцов стали. Из результатов измерения и теоретических моделей механизмов упрочнения расчитаны вклады этих механизмов в общий предел текучести σ. Измеренные величины условного предела текучести $\sigma_{0.2}$ при температуре 350 °C сравниваются с результатами различного сложения отделных вкладов.

1. Introduction

The utilization of the austenitic stainless Ti stabilized steel AISI 321 requests both the corrosion resistance and the long term stability of mechanical properties at moderate temperature of 350 °C. These two properties are influenced by thermo-

*) Department of Metal Physics, Charles University, 121 16 Praha 2, Ke Karlovu 5, Czechoslovakia.

mechanical treatment necessary to produce different construction parts and by final solution and precipitation annealing required to enhance integranular corrosion resistance.

Precipitation annealing, moreover, increases the strength of steel, which can drop significantly after solution annealing due to the recovery of dislocation structure and/or recrystallization. It is therefore of great interest to understand the kinetics, structure and composition of precipitated phases and their contribution to the strength. The understanding of the way how individual hardening contributions are combined to obtain the resulting strength is very important in improving both the properties and technology of materials.

The studied steel is a multicomponent system. Single components take part in the hardening either as solutes (substitutional or interstitial solutes) or as a constituens of different phases the formation of which occurs during thermomechanical treatment.

Solid solution hardening has been studied both theoretically and experimentaly on binary alloys and ternary alloys (1–6). Most probable model of solid solution hardening for f.c.c. solid solutions seems to be that proposed by Labusch (1, 5, 7, 8). An extensive experimental study of solid solution hardening in austenitic stainless steels [3, 9–12) showed that the greatest effects have interstitial solutes carbon and nitrogen. Ferrite forming substitutional solutes (Si, W, Mo, V etc.) exert lower effect, while austenite forming substitutional solutes (Mn, Co, Cu, Ni) have very little solid solution hardening effect.

The empirical equation enabling calculation of proof stress of steel from its chemical composition has been received from experimental studies of steel strengthening (3, 9, 12). Unfortunately, there does not exist any theoretical model of strengthening corresponding to the empirical formulae. The thorough discussion of solution hardening in α-iron by Leslie (13) cannot be easily applied to f.c.c. austenitic steel.

Phase morphology has shown that formation of primary precipitates takes place both during solidification and cooling down of ingots. Mainly TiC, TiN and/or combined Ti(C, N) with varying carbon concentration together with titanium sulphides Ti_2S and/or $Ti_4C_2S_2$ were observed (14, 15). These precipitates do not dissolve even during long solution annealing at 1350 °C.

Fine TiC and/or Ti(C, N) precipitates originate in supersaturated solid solution during annealing at lower temperatures together with another phases, e.g. $(Fe, Cr)_{23}C_6$, $(Ti, Ni)_6C$ and intermetalic phases of Fe–Cr system – σ and χ (14–18). Fine Ti(C, N) particles precipitate in rows along dislocations lines or at stacking faults [19, 20]. Undersirable $M_{23}C_6$ nucleates preferably on grain boundaries, but was observed inside of grains, too [19, 20]. Table I gives an overview of these phases.

There is not yet any experimental study concerning comparison of quantitative characteristics of precipitates in AISI 321 steel (eg. size, fraction volume, shape etc.) with calculated and experimental values of flow stress. It is purpose of the present paper to study precipitation in the steel by means of transmission electron microscopy

and electron diffraction of thin foils and to determine the contribution of single hardening processes involved in final mechanical strength.

Table I.

Phase	Structures	Lattice parm. (nm)
TiC	B1 (NaCl)	a = 0.432
TiN	B1 (NaCl)	a = 0.424
$(TiNi)_6C$	F.C.C.	a = 1.1195
		resp. 1.104
Ti_2S	hex.	a = 0.321
		c = 1.119
$Ti_4C_2S_2$	hex.	a = 0.321
		c = 1.120
$(Fe, Cr)_{23}C_6$	$D8_4$ cub.	a = 1.064
matrix	F.C.C.	a = 0.359

2. Experimental

2.1. Experimental procedure

The precipitation of minority phases during thermomechanical treatment has been studied both by direct observation of the microstructure by transmission electron microscopy (TEM) of thin specimens and by the measurement of resulting mechanical properties (namely proof stress $\sigma_{0,2}$) at 350 °C.

The composition of the steel which is equivalent to AISI 321 austenitic stainless steel used in this experiment is given in table II.

Table II.

Chemical composition of the studied steel

Element	C max.	Mn max.	Si max.	Cr	Ni	Ti max.	C
wgt %	0.06	1.50	0.06	17—19	10—11	0.6	0.3

Material was supplied in the cylinder form after forging at 950 °C. Specimens for tensile tests and TEM have been mechanically grinded and afterwards treated as follows:

1. All specimens have been annealed either at 1200 °C (spec. A) or at 1050 °C (spec. B) for 2 hours and quenched into water (so called solution annealing – SA);

2. One set of specimens was annealed at 750 °C and 800 °C for different periods out to 2 hours – see tables III and IV (so called precipitation annealing – PA).

The other set of specimens was deformed before described PA, namely

spec. (A) 4% at 20 °C,

spec. (B) 8% at 700 °C and 850 °C;

3. One part of specimens has been deformed in the tensile test at 350 °C, the other served for preparation of thin specimens for TEM structure study.

Deformation to determine proof stress has been performed on the INSTRON TT-CL 1195 type testing machine in the Hereaus resistance furnace fixed on the crosshead. Constant crosshead speed equal to 1 mm/s has been used, which corresponds to the average deformation rate of $3 \cdot 10^{-4}\ s^{-1}$. Deformation temperature has been maintained with accuracy ± 5 °C. Deformation preceding PA was carried out at the crosshead speed of 50 mm/s.

PA was performed in argon atmosphere and specimens were water quenched after annealing. The annealing times shown in tables III and IV do not include the time needed to warm up specimen to annealing temperature, which was approximately 10 min.

Microstructure and electron diffraction observation was performed on TESLA BS 540 transmission electron microscope at 120 kV acceleration voltage. Thin slices approx. 0.5 mm thick were spark cut and spark planned to the thickness of about 0.35 mm. Disc with 3 mm diameter were cut by using the same spark erosion method and thined electrochemically to 0.15–0.25 mm in 15 % nitric acid solution in methanol at −30 °C and approx. 5 V (100 mA). Finally disc were polished in automatic jet polishing aparatus TENUPOL using 6% perchloric acid solution in methanol at −40 °C and cell voltage between 35 and 40 V (current 100–150 mA).

2.2. Experimental results

As received and solution annealed steel contains two types of precipitates. The coarse ones are the primary particles of titanium carbides and/or nitrides Ti (C, N) and of titanium sulfides $Ti_4C_2S_2$ (or/and Ti_2S), which precipitated during solidification and following cooling down of ingot and persisted solution annealing at both temperatures used.

The finer secondary particles of Ti(C, N) precipitated in the "cube to cube" orientation (eg. directions ⟨100⟩ of matrix and precipitates are parallel) during treatment of steel prior to this experiment. Secondary precipitates have diameter between 40 nm and 70 nm and are surrounded by dislocation loops. During SA at 1050 °C they mainly persist – fig. 1a and dissolve during SA at 1200 °C – fig. 1b.

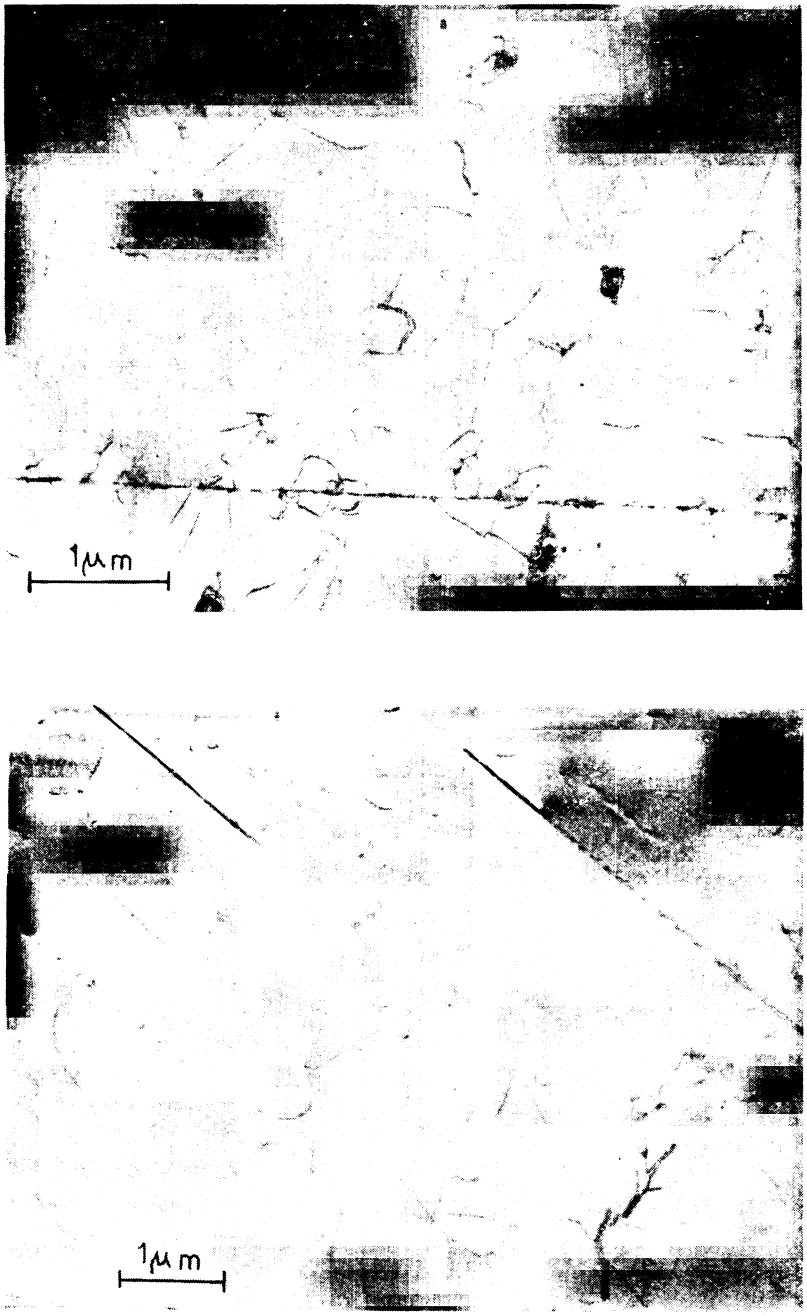

Fig. 1a — Secondary Ti(C, N) precipitates in (B) steel persisting after SA at 1050 °C. *b* — Structure of (A) steel (after SA at 1200 °C).

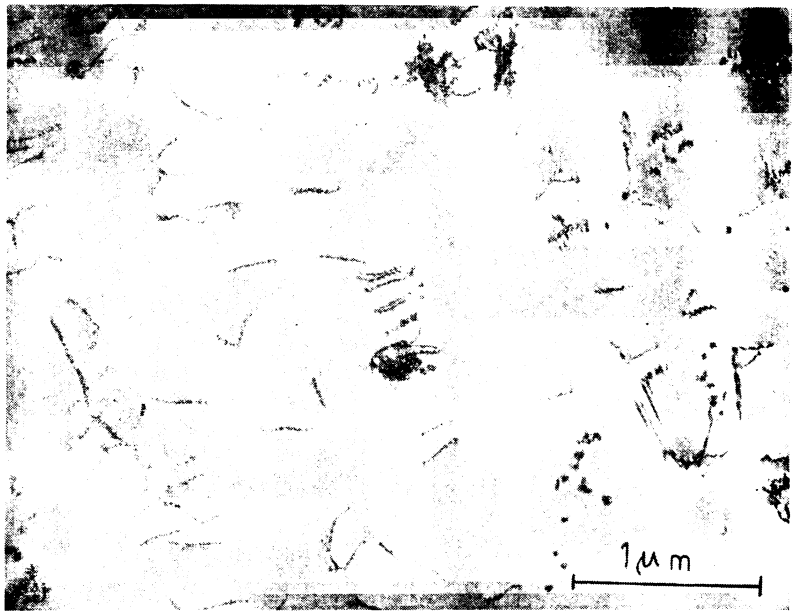

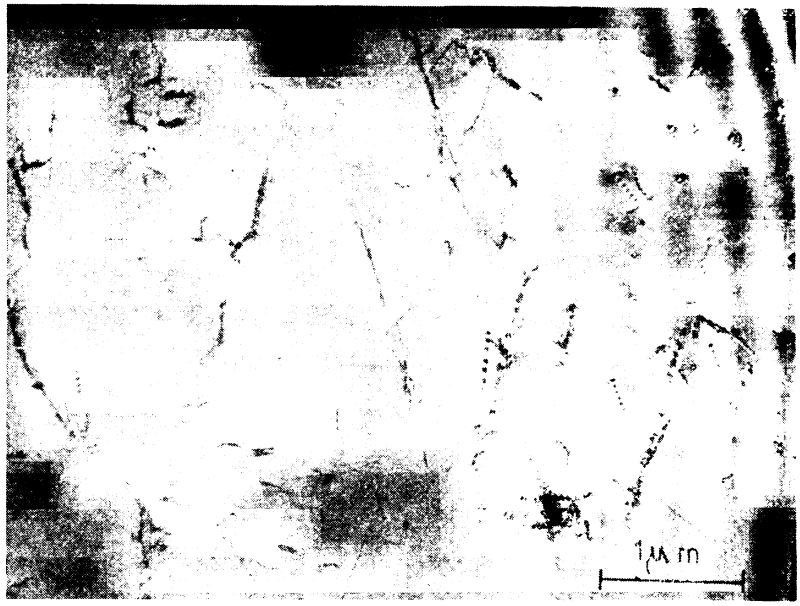

Fig. 2a — Fine Ti(C, N) precipitates in (A) steel after PA at 750 °C for 120 min. *b* — The same after PA at 800 °C for 60 min.

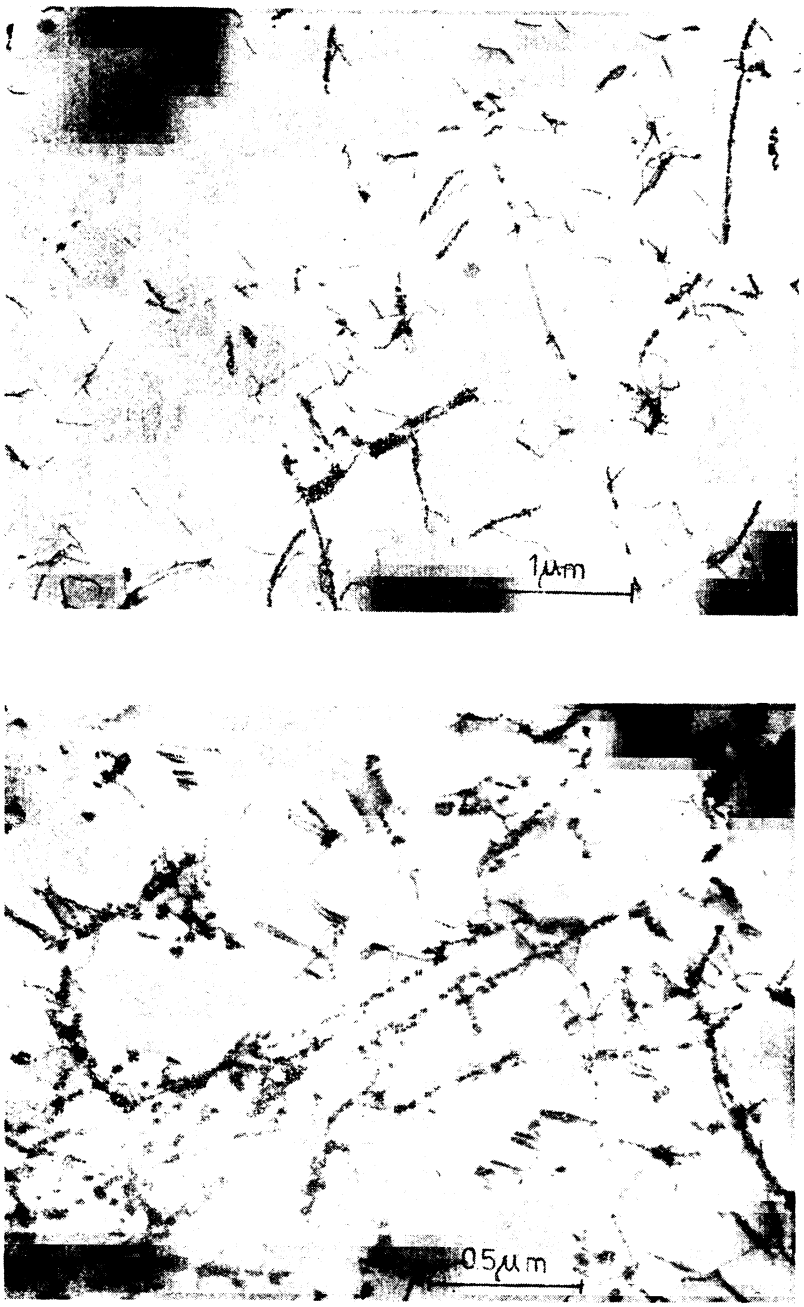

Fig. 3a — Chaining of fine Ti(C, N) particles along dislocation lines in (A) steel after 360 min. PA at 750 °C. *b* — As in a) after 120 min. PA at 800 °C.

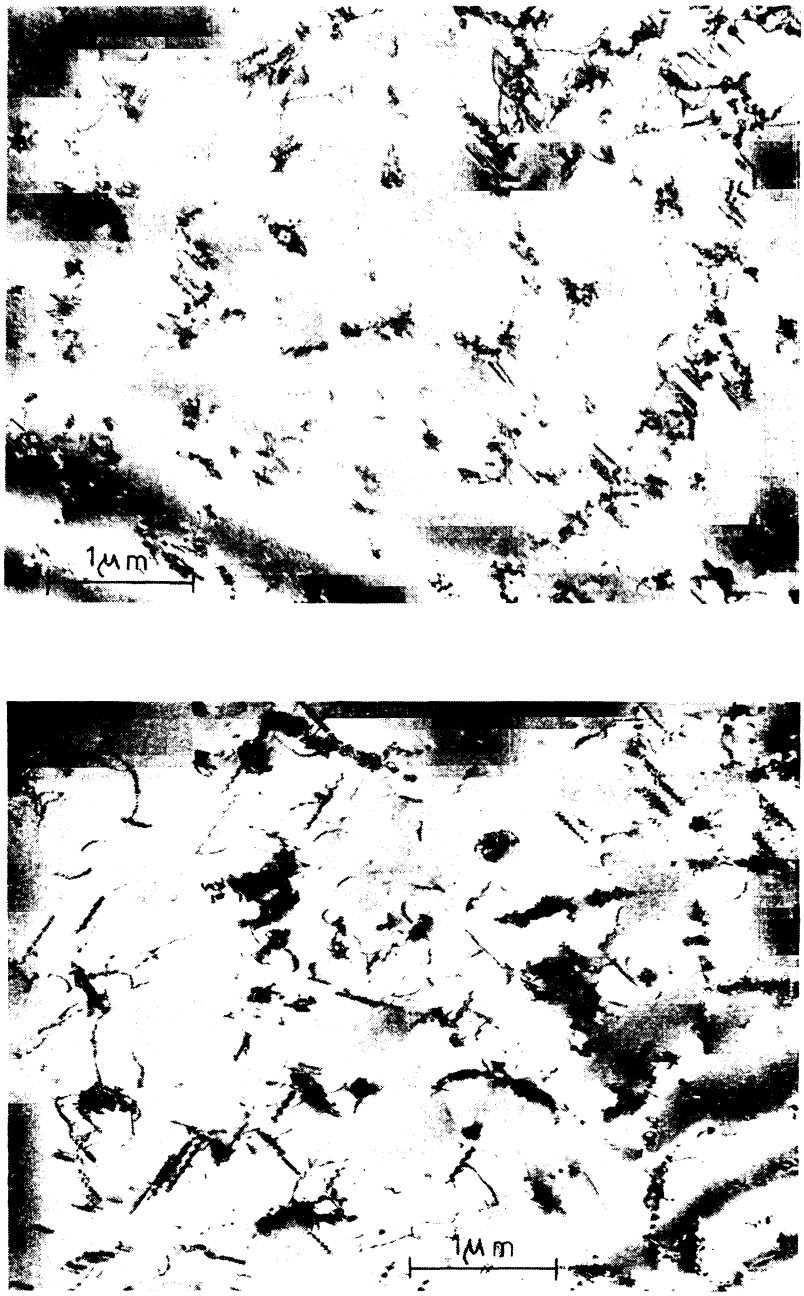

Fig. 4a — Plate-like Ti(C, N) precipitates in steel (A) after 20 hours PA at 750 °C. *b* — As in a) after 24 hours PA at 800 °C.

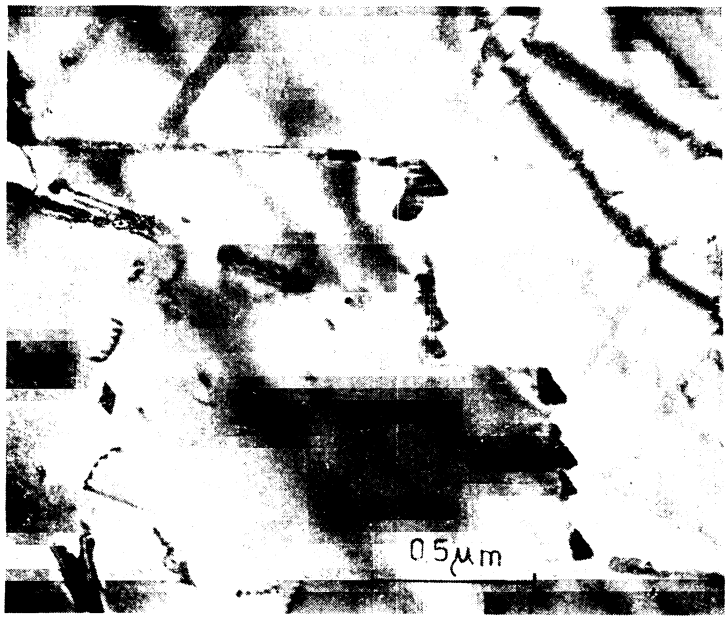

Fig. 5 — $M_{23}C_6$ particles observed in the grain boundary of (A) steel after 60 min. PA at 800 °C.

SA on different temperatures results in different grain size, eg. 100 μm for the (A) steel and 20 μm for the (B) one.

Figs. 2 to 5 illustrate the development of precipitation structure during PA at 750 °C and 800 °C in the (A) steel. The fine spherical particles of Ti(C, N) in the "cube to cube" orientation nucleate and grow along dislocation lines, the tendency of transition from spherical to cubic shape is observed. Plate shaped precipitates of Ti(C, N) originating probably due to chaining of fine particles are observed after longer ageing (20 hours at 750 °C and 2 hours at 800 °C – fig. 4a and 3b resp.). Measured values of particle sizes and densities are summarised in table III. After one hour PA at both temperatures the precipitates $M_{23}C_6$ were occasionally observed in grain boundaries – fig. 5.

The similar precipitation structure development has been observed in steel (B) during PA at 800 °C – figs. 6 and 7. Pronounced formation of plate and needle shaped precipitates is characteristic for steel (B). No $M_{23}C_6$ precipitates were observed. Results obtained for (B) steel are summarised in table IV.

Deformation before PA introduces high dislocation density thus increasing number of nucleation centers. 8% deformation at 700 °C (low temperature one) generates typical dislocation cell structure. PA at 800 °C then results in high density of fine Ti(C, N) precipitates nucleated on dislocation lines – fig. 8a. Neither density nor size of particles changes substantially with prolongated PA but this leads to the precipitation of needle shaped particles – fig. 8b.

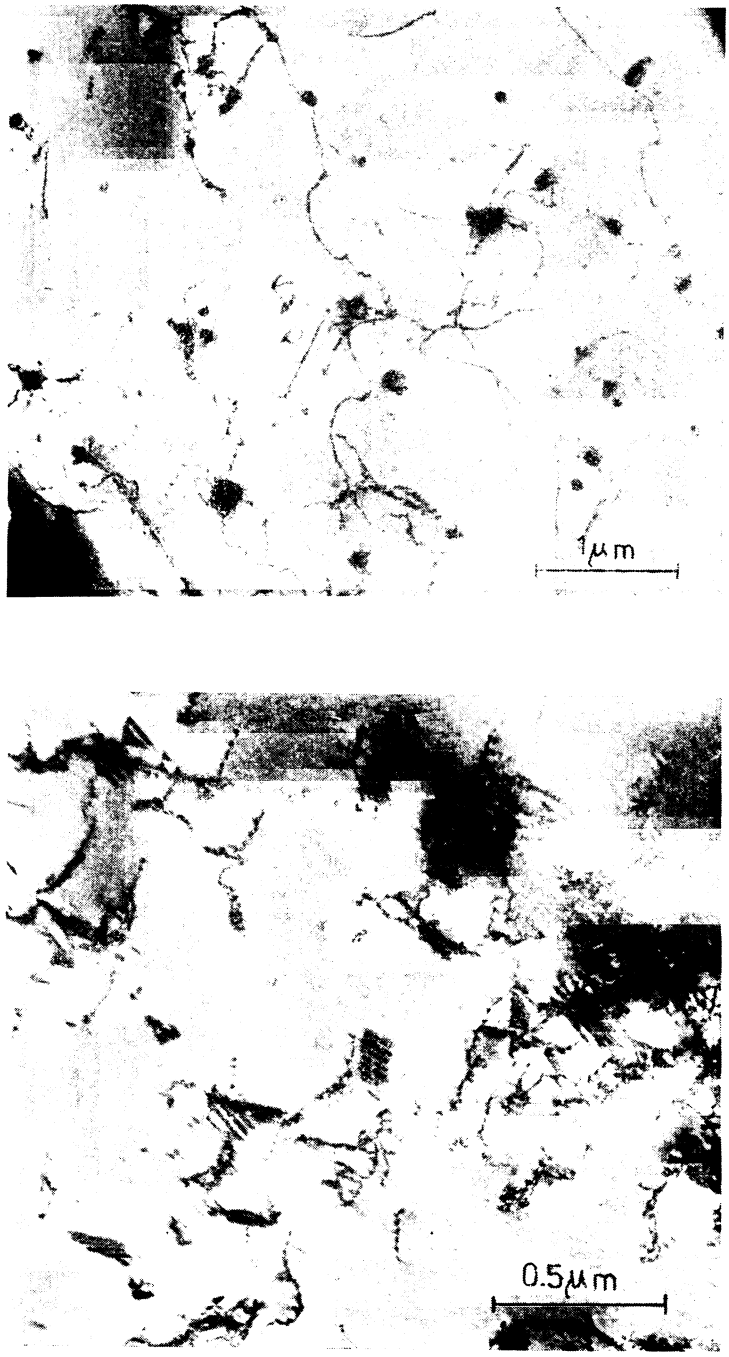

Fig. 6a — Microstructure of (B) steel after 30 min. PA at 800 °C. *b* — Formation of plate-like Ti(C, N) in steel (B) after PA at 800 °C for 120 min.

Fig. 7a — Plate-like precipitates in (B) steel after 360 min. PA at 800 °C. *b* — Needle-like precipitates in the same treated specimen.

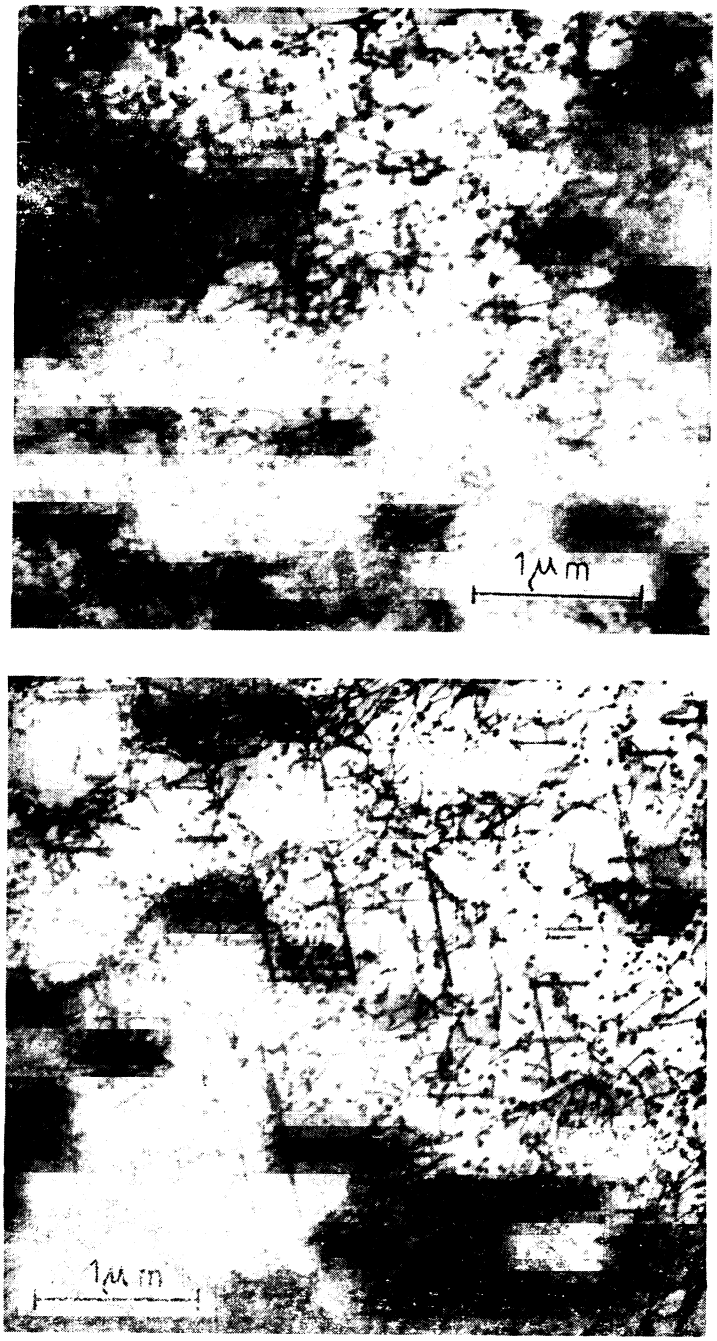

Fig. 8a — Structure of (B) steel after 8% deformation at 700 °C and 120 min. PA at 800 °C (fine spherical Ti(C, N)). *b* — Fine spherical and needle-like particles in the same deformed specimen after 360 min. PA at 800 °C.

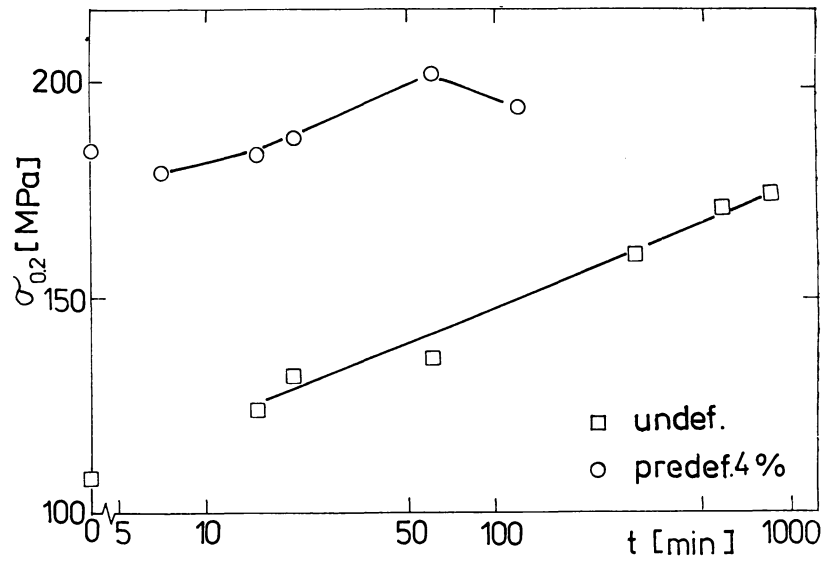

Fig. 9. — The effect of ageing time at 800 °C on the proof stress $\sigma_{0.2}$ of steel (A) obtained at 350 °C (predeformation was carried out at 20 °C).

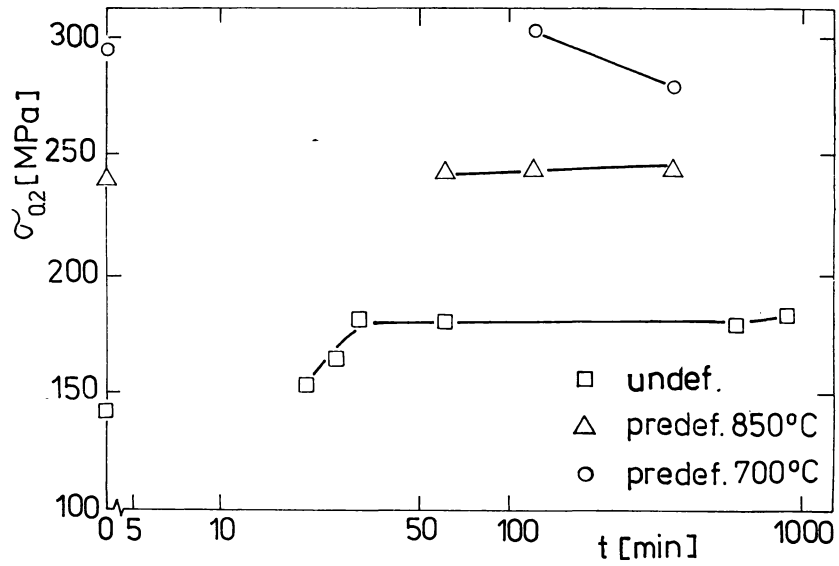

Fig. 10 — The proof stress $\sigma_{0.2}$ dependence of (B) steel at 350 °C on the PA time at 800 °C.

Dislocation arrangement after 8% deformation at 850 °C is characterized by lower dislocation density. This results in the lower density of coarser spherical Ti(C, N) particles.

The dependences of proof stress $\sigma_{0.2}$ at 350 °C on annealing time are plotted in figs. 9 and 10 (some mechanical tests were carried out as a part of diploma works supervised by the author [32, 33]). Linear increase of $\sigma_{0.2}$ with annealing time was observed for steel (A), preliminary deformation at 20 °C decreases the slope of increase – fig. 9. For steel (B) the proof stress increases rapidly after short annealing (shortening of incubation period) and is constant for annealing longer than 30 min. – fig. 10. Preliminary deformation at 850 °C causes complete independency of $\sigma_{0.2}$ on annealing time. The same conclusion can be drawn for steel (B) after deformation at 700 °C, only slight decrease of proof stress was observed for long annealing – fig. 10.

3. Discussion

3.1. Effect of thermomechanical treatment on nucleation and growth of precipitates

Development of precipitate structure in both steel specimen types studied corresponds well with the previous results of other researchers [14, 16, 17, 20–24]. Within accuracy attainable in determination of lattice parameters from selected area electron diffraction the secondary precipitates in (A) steel were found to be Ti(C, N) ones with prevailing content of nitrogen – lattice parameter $a = 0.426$ nm. In (B) steel carbon is majority element in these precipitates. The observed difference can be accounted for by difference in nitrogen and/or carbon content partly also due to higher SA temperature for (A) steel and subsequent $(Cr, Fe)_{23}C_6$ precipitation.

Formation of the latter carbide is probably caused by higher content of dissolved carbon after annealing at 1200 °C then after that at 1050 °C. Volume fraction of $M_{23}C_6$ is very low, only a few grain boundaries were found to contain these carbides. Their nucleation and growth is dependent on local inhomogenities in content of Ti, C and Cr.

The density of fine Ti(C, N) increases for both PA temperatures, reaches maximum and drops again – fig. 11. Size of particles grows with annealing time – fig. 12 according to the expression [25]:

$$t \sim d^n . \tag{1}$$

Exponent n equals 4 and 3 for annealing temperature of 750 °C and 800 °C respectively. Value $n = 3$ corresponds to the growth controlled by difussion processes, the higher value of n at 750 °C shows the slowing down of growth process. For both temperatures of PA the fraction volume of fine carbide Ti(C, N) increases with annealing time – fig. 13. The normalized fraction volume $x = f/f_{max}$ follows Avrami's equation for PA at 800 °C – fig. 13.

$$x = 1 - \exp(-k \, . \, t^m) , \tag{2}$$

where experimental value of $m = 1.42$ is near to the theoretical one for growth of spherical particles ($m_{sph} = 1.5$) [26].

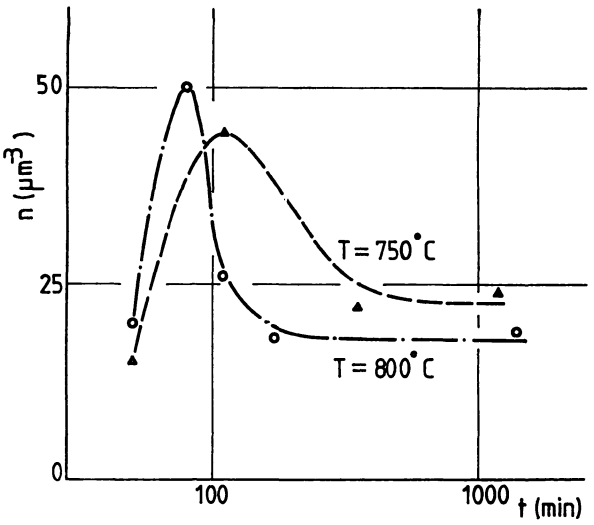

Fig. 11 — Plot of fine Ti(C, N) volume density n in (A) steel versus PA time.

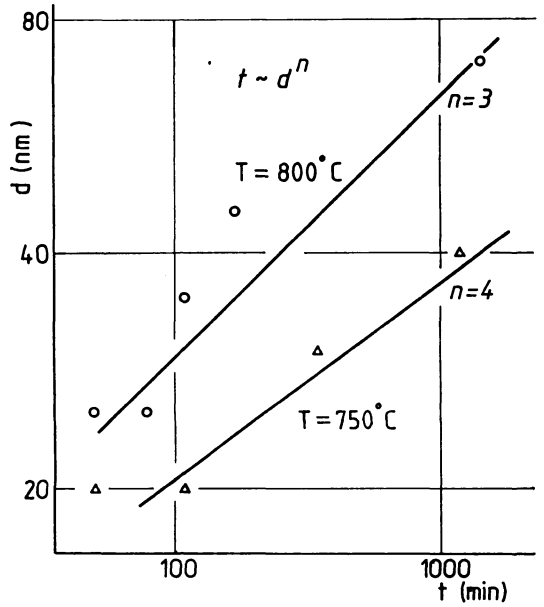

Fig. 12 — Growth of fine Ti(C, N) particle size with PA time in (A) steel.

3.2. Effect of microstructure on mechanical properties

The hardening due to mechanical treatment is the main strengthening mechanism in the studied steel. Nevertheless, the final value of proof stress $\sigma_{0.2}$ is determined by the combination of following strengthening mechanisms:

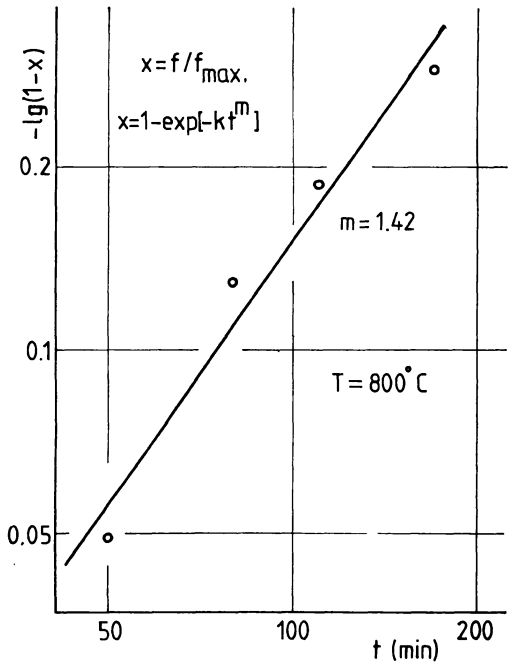

Fig. 13 — Plot of normalized fraction volume of fine Ti(C, N) particles versus PA time (steel (A)).

a) work hardening

The following well known relation between critical resolved shear stress and dislocation density can be used to evaluate this contribution [27] (applied to polycrystals)

$$\sigma^D = 3.1\alpha\mu b\varrho_d^{1/2}\,, \tag{3}$$

where μ is a shear modulus, b is a magnitude of the Burger's vector of dislocation with the density of ϱ_d, α is a geometrical constant and 3.1 is the value of Taylor's factor (taking number of available slip systems into account) for f.c.c. structure.

b) solution hardening

The contribution of i-th single element with atomic concentration c_i can be evaluated using following expression [16]

$$\sigma_i^S = 3.1\mu Z\varepsilon_i^{4/3}c_i^{2/3}\,, \tag{4}$$

where $Z \sim 0.002$ and ε_i is the parameter of elastic interaction between atom of i-th element and dislocation [8]. The total contribution of all solutes can be summed up as follows [1, 5]

$$(\sigma^S)^{3/2} = \sum_1^n (\sigma_i^S)^{3/2}\,. \tag{5}$$

c) precipitation hardening

The strengthening by non-shearable particles of fraction volume f and diameter d equals [28]

$$\sigma^H = 3.1 A \mu b \ln (d_s/b)\, 1/L_s , \tag{6}$$

where $A \sim 0.156$, $d_s = (2/3)^{1/2}\, d$ and $L_s = [(\pi/f)^{1/2} - 2]\, d_s/2$.

d) hardening by substructures

Both the strengthening by grain boundaries and that by subgrain boundaries can be described by the Hall-Petch's type equation

$$\sigma^{G,SG} = k(d_{G,SG})^{-1/2} , \tag{7}$$

where $d_{G,SG}$ is diameter of grain or subgrain.

Results of evaluation of these contributions are summarized in tables III and IV using following parameter values:

$$b = 0.254 \text{ nm} , \quad \mu = 9.6 \times 10^4 \text{ MPa} , \quad 3.1\alpha = 1$$

in equ. (4); $k \sim 1 - 7 \text{ N mm}^{-3/2}$ is supposed for grains and approx. 10 times lower for subgrains [3, 8, 29, 30].

Table III.

Ageing temp. °C	1200	750				800				
Ageing time min.		50	110	350	1190	50	80	110	170	1430
n (μm^{-3})		15	44	22	24	20	50	26	18	19
d (nm)		20	20	30	40	25	25	35	45	70
f (10^{-4})		0.63	1.84	3.11	8.04	1.64	4.1	5.8	8.5	34.1
L_s (μm)		1.81	1.05	1.21	0.99	1.39	0.87	1.02	1.07	0.81
ϱ_d (10^{13} m^{-2})	0.9	1.6	2.0	2.0	2.0	2.0	3.0	2.0	2.0	2.0
σ^D (MPa)	70	95	110	110	110	110	130	110	110	110
σ^H (MPa)		28	49	46	60	39	62	57	57	82
σ^S (MPa)	90				50					
$\sigma_{0.2}$ cal. (MPa)	114	111	130	129	135	127	152	134	134	146
$\sigma_{0.2}$ exp. (MPa)	108	120	146	126	155	132		136	160	174

σ^S was estimated for main solutes C, Cr, Ti, Si and N. The value equals to 90 MPa for (A) steel and 77 MPa for (B) one if Ti, C, N are in solid solution. The corresponding values are 50 MPa and 44 MPa if those three solutes are in precipitates with maximum volume fraction [3, 22].

Precipitation hardening contributions were calculated from experimental values of precipitates size, density and volume fraction (see tables III, IV).

Table IV.

Def. temp. °C	Undeformed					700			850	
ageing temp. °C	1050					800				
ageing time min.	120	30	120	360	0	120	360	0	120	360
n (μm^{-3})	0.6	8			0.6	124	450		107	296
d (nm)	200	100				20	25		40	30
f (10^{-4})	24	42				5.2	37		36	42
L_s (μm)	2.77	1.04				0.62	0.28		0.45	0.31
ϱ_d (10^{13} m^{-2})	1.0	0.92	1.6	1.9	*)	6.7	4.2	6.9	6.6	5.8
σ^D (MPa)	77	74	92	106	>137	199	158	202	198	185
σ^H (MPa)	27	66	> 27	> 27	27	80	187	27	128	173
σ^S (MPa)	77		44		77	44		77	44	
$\sigma^{G,SG}$ (MPa)					35					
$\sigma_{0.2}$ cal. (MPa)	118	114	>111	>123	>180	221	251	220	242	260
$\sigma_{0.2}$ exp. (MPa)	133	181	181	181	294	303	279	240	240	244

*) cell structure — $\Phi = 0.3$ μm

The comparison of the linear sum of contributions with experimentally measured values shows the inadequacy of this procedure. The best agreement with experimental value of $\sigma_{0.2}$ can be obtained by so called "quadratic summing" of contributions [31, 5, 28]

$$\sigma_{0.2}(\text{calc.}) = \{(\sigma^D)^2 + (\sigma^H)^2 + (\sigma^S)^2\}^{1/2} . \tag{8}$$

In the case of (B) steel the $\sigma^{G,SG}$ has been quadratically added, too.

4. Summary

1. Precipitation annealing of AISI 321 steel at 750 °C and 800 °C results in formation of fine secondary Ti(C, N) precipitates on dislocations and other lattice defects. They grow with annealing time and partly change to the needle-like and plate-like shapes.

2. Diffusion processes control the growth of fine secondary precipitates. Fraction volume growth follows the Avrami's equation, the shape of particles is approximately the spherical one.

3. Ti(C, N) stabilizes the anticorrosion properties of steel by restricting the formation of $M_{23}C_6$, unless the temperature of solution annealing is high enough to allow substantial dissolution of primary precipitates of TiC and Ti(C, N).

4. Precipitation strengthening due to secondary Ti(C, N) contributes significantly to the AISI 321 steel strength.

5. The single hardening mechanisms in the studied steel are to be combined quadratically to account for entire strength.

Acknowledgement. The author is indebted to prof. Dr P. Kratochvíl for suggesting the problem and fruitful discussions and to ing. Petrman (SONP POLDI Kladno steel works) for material supplying.

References

[1] Labusch, R.: Phys. stat. sol. 41, 1970, 659.
[2] Kratochvíl, P., Lukáč, P.: Kovové materiály 10, 1972, 180.
[3] Irvine, K. J. et al.: JISI 207, 1969, 1017.
[4] Haasen, P.: Trans. JIM Suppl. 8, 1968, 40.
[5] Friedrichs, J., Haasen, P.: Phil. Mag. 31, 1975, 863.
[6] Gypen, L. A., Deruyttere, A.: J. Mat. Sci. 12, 1977, 1028, 1034.
[7] Jax, P., Kratochvíl, P., Haasen, P.: Acta Met. 18, 1970, 237.
[8] Smola, B.: Czech. J. Phys. B 31, 1981, 447.
[9] Pickering, F. B.: International Metals Rev. 211, 1976, 227.
[10] Irvine, K. J.: JISI 199, 1961, 153.
[11] Holmes, B., Dyson, D. J.: JISI 208, 1970, 469.
[12] Pickering, F. B.: Metallurgical achievements, Pergamon Press, 1965, p. 109.
[13] Leslie, W. C.: Met. Transactions 3, 1972, 5.
[14] Leitnaker, J. M., Bentley, J.: Met. Transactions 8A, 1977, 1605.
[15] Padilha, A. F. et al.: Journ. of Nuclear Materials 105, 1982, 77.
[16] Spektor, J. I. et al.: Metaloved. term. obrab. met. 1, 1970, 39.
[17] Smirnov, M. A. et al.: ibid 1, 1970, 29.
[18] Bourgeot, J. et al.: Mem. Sci. Rev. Metallurgie 72, 1975, 9.
[19] Thorwaldsson, T., Dunlop, G. L.: Metal Sci. 16, 1982, 184.
[20] Thorwaldsson, T., Dunlop, G. L.: ibid 14, 1980, 513.
[21] Kratochvíl, P., Smola, B., Petrman, I.: Hutnické listy 38, 8, 1983, 565
[22] Kratochvíl, P., Smola, B., Petrman, I.: ibid 42, 3, 1987, 188.
[23] Box, S. M., Wilson, F. G.: JISI 210, 1972, 718.
[24] Grot, A. S., Spruiel, J. E.: Met. Transactions 6A, 1975, 2023.

[25] GIRR, M. B., LEE, S. Y.: Proc. of 6-th ICSMA, Melbourne, 1982, 977.
[26] WERT, C., ZENER, C.: J. Appl. Phys. 21, 1950, 5.
[27] KELLY, A., NICHOLSON, R. B. in: Strengthening methods in crystals, ed. Kelly, A. and Nicholson R. B., Appl. Sci. Publ., London, 1971, p. 1.
[28] BROWN, L. M., HAM, R. K. in: Strengthening methods in crystals, ed. Kelly A. and Nicholson R. B., Appl. Sci. Publ., London, 1971, p. 9.
[29] NABARRO, F. R. N. et al.: Adv. Phys. 13, 1964, 193.
[30] ELFMARK, J.: Hutnické listy, 33, 10, 1978, 714.
[31] FOREMAN, A. J. E., MAKIN, M. J.: Canad. J. Phys. 45, 1967, 511.
[32] KUČERA, Z.: Diploma work, Charles University, Faculty of Mathematics and Physics, Prague, 1983.
[33] KARLÍK, M.: Diploma work. Charles University, Faculty of Mathematics and Physics, Prague, 1984.